STUDY ON THE MODEL OF CONTAMINANT IONS REACTION AND DIFFUSION NEAR WELLBORE

by

Xiang-Chao SHI*, Wu-Qiang CAI, and Ying-Feng MENG

State Key Laboratory of Oil and Gas Reservoir Geology and Exploitation,
Southwest Petroleum University, Chengdu, China

Original scientific paper
DOI: 10.2298/TSCI15S1S57S

During the development of oil field, well operation fluids will inevitably invade the formation, and insoluble is produced when contaminant ions contained in operation fluids react with formation fluids, which will easily plugs the pores, consequently affecting the flow of formation fluids. It is of remarkable significance for formation damage evaluation to study the laws of contaminant ions transportation and distribution near wellbore. In this study, the characteristics of high-speed percolation and contaminant ions diffusion near wellbore are reasonably considered, and then we established the non-Darcy flow reaction-diffusion equations, from which the contaminant ions distribution and transportation will be illustrated, thereby, the effects of pollutants migration and reaction on porosity and permeability are further studied. Thus, the newly developed model can provide theoretical basis and practical reference for plug removal.

Key words: contaminant ions, formation damage, non-Darcy flow, reaction-diffusion equations, pollutants migration

Introduction

Well operation fluids invade the formation in the process of oil field development, and react with contaminant ions contained in formation fluids, which will easily produce insoluble and lower the formation permeability. To provide a reference for plug-removal measures, it is essential to accurately predict the laws of underground water seepage and contaminant ions transportation and distribution, which will bring huge benefits [1-4].

For the porous media seepage model established based on the Darcy law, a viscosity term should be considered when study the high speed percolation. Brinkman and Forchheimer [5] modified the Darcy law by adding the inertia force item and viscosity term. Beckermann [6] solved the coupling model of laminar layer and porous medium using the Brinkman-Forchheimer equation, through which the problem of natural convection and heat transfer in coupling field was worked out. In this paper, we take the features of high-speed percolation near wellbore into consideration and utilize Darcy-Forchheimer nonlinear equations, and then establish the model of pollutants distribution and migration, sequentially, the characteristics of porosity and permeability of the formation near wellbore can be predicted through the numerical results.

* Corresponding author; e-mail: sxcdream@163.com; cwctmyf@vip.sina.com

Establishment of percolation model

Model hypothesis

The pollution ions in oilfield development process include [1, 7, 8]: Ca^{2+}, Ba^{2+}, Mg^{2+}, Sr^{2+}, CO_3^{2-}, SO_4^{2-}, *etc*. Some precipitations like $CaCO_3$, $BaSO_4$, $MgCO_3$, and $SrSO_4$, will be easily generated when formation water and working fluid are mixed. Introduce the symbols A^{2+} and B^{2-}, $A^{2+} = \{Ca^{2+}, Ba^{2+}, Mg^{2+}, Sr^{2+}\}$, $B^{2+} = \{CO_3^{2-}, SO_4^{2-}\}$, and the precipitations can be expressed as AB.

There are enough ions A^{2+} within the near-wellbore formation, and with the incompressible steady flowing, it supplements into column core through rectangle hole, then mixed with B^{2-} and precipitation AB is generated. According to nucleation theory, assuming the precipitation reaction is a fourth-order reaction, and then the reaction rate can be expressed by eq. (1) [4, 9]:

$$q = K_a C_A^2 C_B^2 \tag{1}$$

The equivalent diffusion coefficient in porous media can be calculated by

$$D_{\text{pore}} = D^{\text{eff}} = D_{\text{free}} \frac{\varphi}{\tau} \tag{2}$$

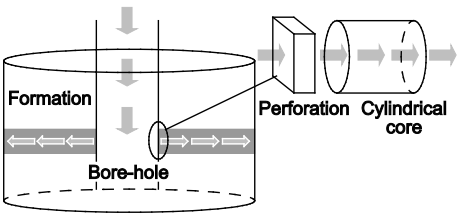

Figure 1. Diagrammatic sketch of coupled flow and field

Equations of flow field control

Diagrammatic sketch of coupled flow field near wellbore is shown in fig.1.

Incompressible fluids flowing through a hole, based on Navier-Stokes equations, we can get:

$$\begin{cases} \dfrac{D(\rho\vec{\mathrm{V}})}{Dt} = -\nabla[-\mu(\nabla\vec{\mathrm{V}} + (\nabla\vec{\mathrm{V}})^T + p_{\text{free}}\mathrm{I}] \\ \nabla\vec{\mathrm{V}} = 0 \end{cases} \tag{3}$$

where I is the unit matrix (a second order tensor), D/Dt – the particle derivative, $D/Dt = \partial/\partial t + \vec{\mathrm{V}}\nabla$.

When flowing through the porous medium, the flow characteristics can be described using Darcy-Forchheimer eq. (4):

$$\vec{\mathrm{V}}^{\text{eff}} = \frac{K(\vec{\mathrm{r}},t)}{\mu}\left[-\nabla p_{\text{Darcy}} + \nabla\frac{\mu}{\phi}(\nabla\vec{\mathrm{V}}^{\text{eff}} + (\nabla\vec{\mathrm{V}}^{\text{eff}})^T\right] \tag{4}$$

where $\vec{\mathrm{r}}$ is the radius vector.

The requirement of flow field coupling is that there exits the same velocity and the same pressure on the interface of two fluids [5], shown in eq. (5):

$$\begin{cases} \vec{\mathrm{V}}^{\text{eff}}\Big|_{\partial\Omega'} = \vec{\mathrm{V}}\Big|_{\partial\Omega'} \\ p_{\text{free}}\Big|_{\partial\Omega'} = p_{\text{Darcy}}\Big|_{\partial\Omega'} \end{cases} \tag{5}$$

where $\partial\Omega'$ is the interface of the hole and core on inlet and outlet.

Under the rectangular co-ordinate system, eq. (3) can be converted into eq. (6):

$$\begin{cases} \dfrac{\partial \rho (V_x V_y)^T}{\partial t} = \nabla_{x,y} \begin{bmatrix} \begin{pmatrix} 2\mu & 0 \\ 0 & \mu \end{pmatrix} & \begin{pmatrix} 0 & 0 \\ \mu & 0 \end{pmatrix} \\ \begin{pmatrix} 0 & \mu \\ 0 & 0 \end{pmatrix} & \begin{pmatrix} \mu & 0 \\ 0 & 2\mu \end{pmatrix} \end{bmatrix} \nabla_{x,y} \vec{\mathrm{V}} - \left(\dfrac{\partial p_{\text{free}}}{\partial x} \dfrac{\partial p_{\text{free}}}{\partial y} \right)^T - \rho \begin{bmatrix} V_x \dfrac{\partial V_x}{\partial x} + V_x \dfrac{\partial V_y}{\partial y} \\ V_y \dfrac{\partial V_x}{\partial x} + V_y \dfrac{\partial V_y}{\partial y} \end{bmatrix} \\ \nabla \vec{\mathrm{V}} = 0 \quad \Rightarrow \quad \dfrac{\partial V_x}{\partial x} + \dfrac{\partial V_y}{\partial y} = 0 \end{cases} \tag{6}$$

Boundary conditions of flow field

The injection side keeps a constant flow rate, and the pressure at outlet end equals to the ambient pressure, that is:

$$\begin{cases} V_{\text{in}} = V_0 \\ p_{\text{out}} = p_0 \end{cases} \tag{7}$$

Equations of ion concentration control

Ions concentration distribution in porous media flow field follows convective-diffusive eq. (8):

$$\begin{cases} \dfrac{\partial c_B}{\partial t} = \tilde{D} \dfrac{\partial^2 c_B}{\partial x^2} + \tilde{D} \dfrac{\partial^2 c_B}{\partial y^2} - \tilde{V} \dfrac{\partial c_B}{\partial x} - \tilde{V} \dfrac{\partial c_B}{\partial y} - q \\ \dfrac{\partial c_A}{\partial t} = \tilde{D} \dfrac{\partial^2 c_A}{\partial x^2} + \tilde{D} \dfrac{\partial^2 c_A}{\partial y^2} - \tilde{V} \dfrac{\partial c_A}{\partial x} - \tilde{V} \dfrac{\partial c_A}{\partial y} - q \\ \dfrac{\partial c_{AB}}{\partial t} = q \\ \tilde{D} = aD + bD^{\text{eff}}, \quad \tilde{V} = aV + bV^{\text{eff}} \end{cases} \tag{8}$$

where a and b are logic parameters, take 0, 1 in cores, and 1, 0 in perforations, respectively, and q is four order reaction rate, [mol·m^{-3}s^{-1}].

Initial condition of ion concentration

Initial condition of ions concentration is as eq. (9):

$$\begin{cases} c_A\big|_{t=0} = c_{A0} \\ c_B\big|_{t=0} = c_{B0} \end{cases} \tag{9}$$

where c_{A0} [molm^{-3}] is the origin ion concentration of A^{2+}, and c_{B0} [molm^{-3}] – the ion concentration of B^{2-} in operation fluid at injection side of rectangular hole.

Boundary condition of ions concentration

Treat the perforation midpoint of wellbore as the origin of co-ordinates, creating a co-ordinate system as shown in fig. 2.

The boundary condition of A^{2+} and B^{2-} is:

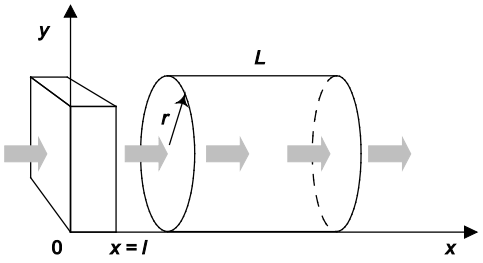

Figure 2. Cylindrical core and co-ordinate axis

$$\begin{cases} c_A\big|_{x=l} = c_{A0} \\ c_B\big|_{x=0} = c_{B0} \end{cases} \tag{10}$$

where $x = 0$ is the left border of the entrance hole, $x = l$ [m] – the right border of the entrance hole (cylindrical core left end), l [m] – the the length of entrance hole; L and r [m] are the length and diameter of cylindrical core, respectively.

Distribution of porosity and permeability

Contaminant ions combine together and generate insoluble, and porosity and permeability are reduced. The porosity can be calculated by eq. (11):

$$\frac{\mathrm{d}\varphi}{\mathrm{d}t} = -\frac{\varphi q}{M_{AB}^{-1}\ \rho_{AB}} \tag{11}$$

where M_{AB} and ρ_{AB} are the molar mass and density of precipitate AB, respectively.

Adler [10] concluded the power law relationship between porosity and permeability, which can be seen as eq. (12):

$$K(\vec{\mathrm{r}},t) = k\varphi^n \tag{12}$$

where k is constant, considering the slippage effect, take $n = 3.55$ [11]:

$$K(\vec{\mathrm{r}},t) = K^0(\vec{\mathrm{r}},t)\left(\frac{\varphi}{\varphi^0}\right)^{3.55} \tag{13}$$

Table 1. Parameters of flow

u_0 [ms^{-1}]	p_0 [Pa]	D [m^{2}s^{-1}]	D^{eff} [m^{2}s^{-1}]	$K^0(\vec{\mathrm{r}},t)$ [mD]
$1.5\cdot10^{-4}$	0	$2.7\cdot10^{-8}$	$2.7\cdot10^{-9}$	170
ρ_{AB} [kgm^{-3}]		c_{A0} [mgL^{-1}]	c_{B0} [mgL^{-1}]	μ [cP]
4520		230	2800	1.0

Table 2. Geometrical parameters of the rock hole

l [m]	L [m]	φ^0 [%]	r [m]
0.4	0.4	30	0.1

where $K^0(\vec{\mathrm{r}},t)$ [m^2] is the initial distribution of permeability, and φ^0 [%] is the initial distribution of porosity.

Case study

Basic data

The basic parameters used to calculate are shown in tabs. 1 and 2.

The reaction rate constant of dynamic scaling is proportional to the velocity, seen as eq. (14):

$$K_4 = \lambda V^{\mathrm{eff}}\varphi \tag{14}$$

At a flow rate of $1.5\cdot10^{-4}$ m/s and the chemical reaction intensity coefficient is of $0.149\cdot10^9$ [(mol·L^{-1})^{3}m]$^{-1}$, gets $K_4 = 6.7\cdot10^{-6}$ m^9(s·mol^3)$^{-1}$.

Numerical solution of dynamic changes in porosity and permeability

The properties of porosity and permeability change dramatically with the contact time of operation fluids and formation fluids. Figures 3 and 4, and tab. 3 show the porosity and permeability distribution of cylindrical core axial section from $t = 0$ to 60×1 ks.

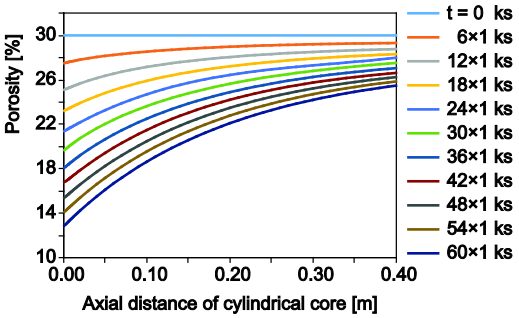

Figure 4. Permeability distribution of the axial section in cylindrical core
(for color image see journal web-site)

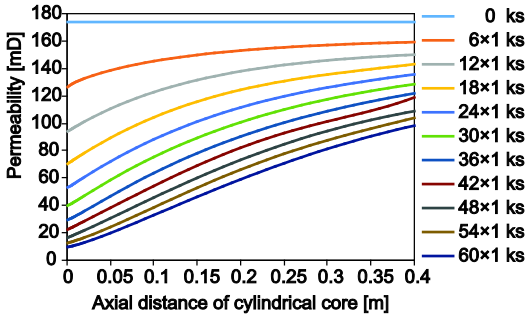

Figure 4. Porosity distribution of the axial section in cylindrical core
(for color image see journal web-site)

$\overline{\varphi}$ and $\overline{K}$ represent the average distribution of porosity and permeability in the axial profile. The calculation methods are defined as:

$$\overline{\varphi} = \frac{1}{L}\int_0^L \varphi(x,t)\,\mathrm{d}x$$

$$\overline{K} = \frac{1}{L}\int_0^L K(x,t)\,\mathrm{d}x \qquad (15)$$

Table 3. The variation of porosity and permeability changes with the injection time

T [ks]	φ [%]	$\overline{\varphi}/\varphi^0$ [%]	K [mD]	$\overline{K}/K^0$ [%]
0	30.00	100.00	174	100
6	28.84	96.1	150.74	86.6
12	27.77	92.6	133.60	76.8
18	26.84	89.5	119.38	68.6
24	25.94	86.5	106.70	61.3
30	25.13	83.8	96.09	55.2
36	24.28	80.9	86.13	49.5
42	23.52	78.4	78.35	45.0
48	22.75	75.8	70.37	40.4
54	22.02	73.4	63.73	36.6
60	21.31	71.0	57.82	33.2

Discussion

Figures 3 and 4 show the dynamic distribution of porosity and permeability of the cylindrical core in time and space. With the injection time increasing, the distributions of porosity in axial profile transition from linear to exponential and, the rate of change in porosity at the end of the injection side is getting smaller. The distribution patterns of permeability in the core axial section are linear and it is sensitive to time. The porosity and permeability change with time equidistantly at the end of injection side and outflow side and the entire flow field tends to be stabilized after 18 ks. It can be concluded that the core with a length of 0.4 m can better reflect the characteristics of porosity and permeability of the formation near wellbore, so the scale of core is appropriately selected.

Conclusions

- Darcy-Forchheimer flow equation is available and feasible for reflecting the flow characteristics of high speed flow near wellbore and, the reaction-diffusion model can better illustrates the nonlinear characteristics of the contaminants migration under flow field coupled.
- The core with a length of 0.4 m can clearly reflect the characteristics of porosity and permeability of the formation near wellbore under the condition of the reaction rate constant $K_4 = 6.7\cdot10^{-6}$ $\mathrm{m}^9(\mathrm{s}\cdot\mathrm{mol}^3)^{-1}$.

- The porosity and permeability at the end of injection side are sensitive to time and the entire flow field tends to be stable after 18 ks (under the given conditions in this paper), which provides a reference for plug-removal measures.

Acknowledgments

The work is supported by the Open Fund (Number: PLN1421) of State Key Laboratory of Oil and Gas Reservoir Geology and Exploitation (Southwest Petroleum University), SWPU Science & Technology Fund (Number: 2013XJZ029), scientific fund of Sichuan provincial education department (Number: 14ZB0060) and CNPC Key Laboratory of Drilling Engineering.

References

[1] Yuan, M. D., Todd, A. C., Prediction of Sulfate Scaling Tendency in Oilfield Operations (includes associated papers 23469 and 23470), *SPE Production Engineering*, *6* (1991), 1, pp. 63-72
[2] Bedrikovetsky, P. G., *et al*., Barium Sulphate Oilfield Scaling: Mathematical and Laboratory Modelling, *Society of Petroleum Engineers*, *1* (2004), ID SPE-87457-MS
[3] Bedrikovetsky, P. G., *et al*., Oilfield Scaling – Part II: Productivity Index Theory, *Society of Petroleum Engineers*, *1* (2003), ID SPE-81128-MS
[4] Bedrikovetsky, P. G., *et al*., Oilfield Scaling – Part I: Mathematical and Laboratory Modelling, *Society of Petroleum Engineers*, *1* (2003), ID SPE-81127-MS
[5] Neale, G., Nader, W., Practical Significance of Brinkman's Extension of Darcy's Law: Coupled Parallel Flows within a Channel and a Bounding Porous Medium, *The Canadian Journal of Chemical Engineering*, *52* (1974), 4, pp. 475-478
[6] Beckermann, C., *et al*., Natural Convection Flow and Heat Transfer between a Fluid Layer and a Porous Layer inside a Rectangular Enclosure, *Journal of Heat Transfer*, *109* (1987), 2, pp. 363-370
[7] Sheikholeslami, R., Ong, H., Kinetics and Thermodynamics of Calcium Carbonate and Calcium Sulfate at Salinities up to 1.5 M, *Desalination*, *157* (2003), 1, pp. 217-234
[8] Smith, P. S., *et al*., Combined Scale Removal and Scale Inhibition Treatments, *Society of Petroleum Engineers*, *1* (2000), ID SPE-60222-MS
[9] Bethke, C., *Geochemical Reaction Modeling: Concepts and Applications*, Oxford University Press., New York, USA, 1996
[10] Adler, P. M., *et al*., Flow in Simulated Porous Media, *International Journal of Multiphase Flow*, *16* (1990), 4, pp. 691-712
[11] Borisova, E. A., Adler, P. M., Deposition in Porous Media and Clogging on the Field Scale, *Physical Review E*, *71* (2005), 1, pp. 16311

Paper submitted: January 20, 2015
Paper revised: February 12, 2015
Paper accepted: February 20, 2015